Applied Mathematics Letters 94 (2019) 80–86

Contents lists available at ScienceDirect

Applied Mathematics Letters

www.elsevier.com/locate/aml

How do dispersal rates affect the transition from periodic to irregular spatio-temporal oscillations in invasive predator–prey systems?

Jamie J.R. Bennett[1], Jonathan A. Sherratt *

Department of Mathematics and Maxwell Institute for Mathematical Sciences, Heriot-Watt University, Edinburgh EH14 4AS, UK

ARTICLE INFO

Article history:
Received 31 October 2018
Received in revised form 14 February 2019
Accepted 14 February 2019
Available online 21 February 2019

Keywords:
Periodic travelling waves
Spatiotemporal irregularity
Invasion
Band width
Predator–prey

ABSTRACT

When one considers the spatial aspects of a cyclic predator–prey interaction, ecological events such as invasions can generate periodic travelling waves (PTWs)—sometimes known as wavetrains. In certain instances PTWs may destabilise into spatio-temporal irregularity due to convective type instabilities, which permit a fixed width band of PTWs to develop behind the propagating invasion front. In this paper, we detail how one can locate this transition when one has unequal predator and prey dispersal rates. We do this by using absolute stability theory combined with a recent derivation of the amplitude of PTWs behind invasion. This work is applicable to a wide range of reaction–diffusion type predator–prey models, but in this paper we apply it to a specific set of equations (the Leslie–May model). We show that the width of PTW band increases/decreases when the ratio of prey and predator dispersal rates is large/small.

1. Introduction

Ecological invasion has become an increasingly common occurrence due to a rise in human activity over the last century; directly because of increased globalisation across commercial industries that lead to the accidental introduction and spread of foreign species, and indirectly through processes such as climate change which drives species into non-native environments [1]. Invasive species threaten native wildlife through predation, outcompeting for resources and spreading disease which ultimately affects ecosystem biodiversity [2]. It is therefore important for the management and control of invasive species to understand not only how invasive populations establish and spread through a new habitat, but also the behaviour of the system in

* Corresponding author.
E-mail address: j.a.sherratt@hw.ac.uk (J.A. Sherratt).

[1] The author's work was supported by The Maxwell Institute Graduate School in Analysis and Its Applications, a Centre for Doctoral Training funded by the UK Engineering and Physical Sciences Research Council (grant EP/L016508/01), the Scottish Funding Council, UK, Heriot-Watt University, UK, and the University of Edinburgh, UK.

https://doi.org/10.1016/j.aml.2019.02.013
0893-9659/

the wake of invasion. One possibility is that an invasive predator–prey interaction is cyclic in nature, which permits the generation of interesting spatial phenomena including PTWs [3–5], where peaks in population density slowly migrate across the habitat. Another type of phenomena observed behind invasion in cyclic systems is spatio-temporal irregularity, which sometimes occurs immediately behind invasion, and sometimes after an initial seemingly stable band of PTWs [6–12]. When PTWs are observed before destabilisation, the band of waves grows before eventually attaining a constant width which we refer to as the band width. Our aim in this paper is to investigate how predator and prey dispersal rates affect the band width of PTWs.

We consider two-component reaction–diffusion models describing predator and prey population densities in space x and time t. The equations for predators $p(x,t)$ and prey $h(x,t)$ are

$$\frac{\partial p}{\partial t} = f(p,h) + \frac{\partial^2 p}{\partial x^2}, \qquad \frac{\partial h}{\partial t} = g(p,h) + \delta\frac{\partial^2 h}{\partial x^2}, \tag{1}$$

where $\delta > 0$ is the ratio of prey and predator dispersal coefficients, and f, g are functions describing the predator–prey interaction. We assume that (1) has at least two homogeneous steady states—an unstable prey-only steady state, and a coexistence steady state. On a one-dimensional finite domain, an invasion of predators therefore corresponds to initially having the unstable prey-only steady state everywhere, except for a small perturbation at one boundary. This induces an invasion front that spreads across the domain at a speed dependent upon model parameters. When, additionally, the coexistence steady state is unstable due to a standard supercritical Hopf bifurcation corresponding to a stable limit cycle, a family of PTW solutions of (1) exist; invasion then selects one of these which can be observed behind the invasion front [13].

A useful property of (1) is that its normal form valid close to a supercritical Hopf bifurcation can be written as the complex Ginzburg–Landau equation (CGLE),

$$\frac{\partial W}{\partial t} = W - (1+i\alpha)\left|W\right|^2 W + (1+i\beta)\frac{\partial^2 W}{\partial x^2}, \tag{2}$$

where W is a complex function of x and t, and α, β are real parameters. Note that (2) is equivalent to the well known λ-ω equations [14] when $\beta = 0$. α and β can be calculated in terms of the model parameters of (1), and the real and imaginary parts of W correspond to weighted sums of predator and prey densities. (2) has a one-parameter family of PTW solutions given by $W = A\exp\left(i\sqrt{1-A^2}x + i\omega t\right)$ where $A = \sqrt{1-Q^2} > 0$ and $\omega = (\beta-\alpha)Q^2 + \alpha$. Therefore, we only require the amplitude of the wave in order to obtain the full solution.

A previous study [15] has detailed how one can locate the transition between regular and irregular spatio-temporal oscillations for the λ-ω (normal form) equations, which allowed the authors to draw conclusions about predator–prey models with equal dispersal rates ((1) with $\delta = 1$). This was possible because of a previously derived equation for the amplitude in terms of parameters which can be found in [16]. A similar study [17] then allowed one to locate this transition point in (2), however, a key shortcoming of that work was that results were not applied to (1). This is because the analogous equation for the amplitude was only derived recently in [18]: when initial conditions are such that a "pulled front" moving with velocity $v^* = 2\sqrt{1+\beta^2}$ develops (this includes invasion initial conditions, see [19] for details) the amplitude can be written in terms of parameters as $A = \left[2\left(\sqrt{(1+\alpha^2)(1+\beta^2)} - (1+\alpha\beta)\right)/(\alpha-\beta)\right]^{1/2}$ [18].

Therefore, subject to normal form rescalings, we can approximate the small amplitude PTW solutions generated by invasion in (1) using (2), with increasing accuracy as the Hopf bifurcation is approached. In Fig. 1, numerical simulations of (2) are shown as density plots in space and time; the previously discussed prey only steady state now corresponds to $W = 0$ and similarly a small perturbation at the left boundary causes a front to propagate across the domain. A change in δ affects the normal form of (1) via the coefficient β; Fig. 1 shows how the propagation speed of the front affects the amplitude of PTWs and therefore the band width observed, as β is varied. In Section 2 we will show how one can calculate the band width of PTWs in the CGLE, and in Section 3 we will fill the gaps of previous studies by determining how predator and prey dispersal affects band width.

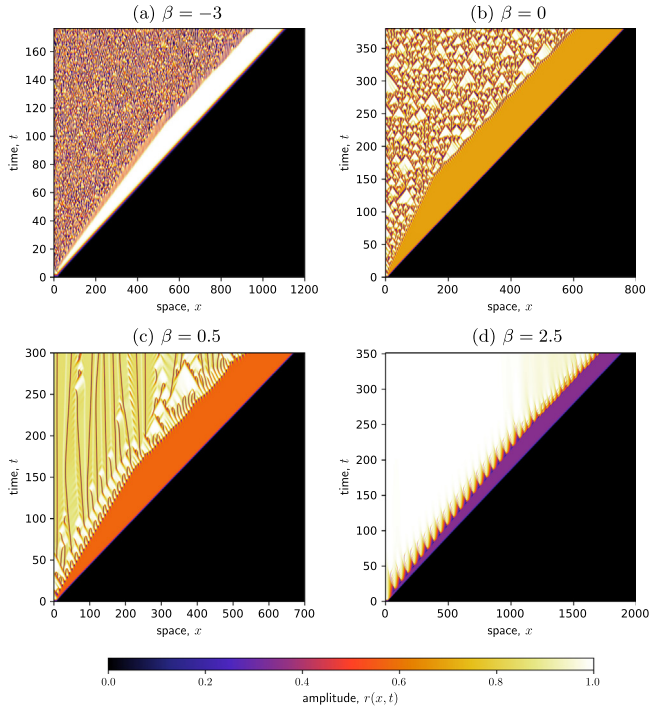

Fig. 1. A band of periodic travelling waves in the complex Ginzburg–Landau equation develops, eventually attaining a fixed band width. We show density plots of $r = \sqrt{\mathrm{Re}(W)^2 + \mathrm{Im}(W)^2}$ for $\alpha = 3$ and β given in the panels. Simulations show different front propagation speed, PTW amplitude and band width. Initially, $W = 0$ everywhere except for a small perturbation made at the left-hand boundary. Eq. (2) was solved using a semi-implicit finite difference scheme with a grid spacing of 0.2 and a time step of 0.005, on a domain with zero flux boundary conditions at both ends.

2. Band width of PTWs in the CGLE

The method described in this section is not novel and so we provide a brief description only, referring the reader to previous work [15,17,20,21]. The first step in calculating the band width is to consider the absolute stability of PTWs in a moving frame of reference; that is, we consider whether small perturbations to the PTW grow or decay when viewed at a fixed point moving with velocity V. If the wave is absolutely unstable in a frame of reference $V \geq v^*$, perturbations can keep pace with the invasion front so that PTWs are not observed at all. Therefore we assume the wave is absolutely unstable in a frame of reference $V < v^*$ so perturbations cannot catch the invasion front, allowing for a regular band of PTWs before destabilising modes dominate the solution leading to spatio-temporal irregularity.

To calculate the band width we first must define its edges; the right-hand edge is just the invasion front, however the left-hand edge is a little more ambiguous—we define it to be the point at which perturbations become amplified by a factor $\mathcal{F}$. We denote $\lambda_{\max}(V)$ to be the maximum growth rate of perturbations in the frame of reference moving with velocity V, and with corresponding wavenumber $k_{\max}(V)$. If we consider a point on the front (x^*, t^*), perturbations spread out from this point in space and time according to $x = x^* + (t - t^*)V$. Linear modes grow like $\mathrm{e}^{\mathrm{Re}[\lambda_{\max}(V)]t}$ so that amplification by a factor $\mathcal{F}$ occurs at $t_{\mathrm{crit}}(V) = t^* + \log(\mathcal{F})/\,\mathrm{Re}\,[\lambda_{\max}(V)]$ at the location $x_{\mathrm{crit}}(V) = x^* + V\log(\mathcal{F})/\,\mathrm{Re}\,[\lambda_{\max}(V)]$. The band width is then the minimum distance between the point (x^*, t^*) and the curve $(x_{\mathrm{crit}}(V), t_{\mathrm{crit}}(V))$ which can be shown [15] to occur at $V = V_{\mathrm{band}}$ given by solving

$$(v^* - V_{\mathrm{band}})\,\mathrm{Im}\,[k_{\max}(V_{\mathrm{band}})] = \mathrm{Re}\,[\lambda_{\max}(V_{\mathrm{band}})]\,. \tag{3}$$

The band width itself is given by

$$\mathcal{L}(\alpha,\beta) = -\log(\mathcal{F})/\operatorname{Im}\left[k_{\max}(V_{\text{band}})\right], \tag{4}$$

see [15]. Notice that $\log(\mathcal{F})$ is parameter independent. For this reason we define the quantity $\mathcal{W} = 1/\operatorname{Im}\left[k_{\max}(V_{\text{band}})\right]$ which we refer to as the band width coefficient.

The key quantity for the band width calculation is $\lambda_{\max}(V)$ and so we now detail how one can obtain it using the theory of absolute stability. First one needs to find the linear dispersion relation, $\mathcal{D}(\lambda,k;V)=0$, by linearising (2) about the exact PTW solution, where α and β are given by a model specific normal form reduction. Substitution of exponential ansatz in the frame of reference $x-Vt$ then yields the expression relating spatial and temporal eigenvalues. $\mathcal{D}(\lambda,k;V)$ is a fourth order polynomial in k, and for a given λ we label its four roots $k_1,\ldots,k_4$ according to the condition $\operatorname{Im}(k_1)\leq\operatorname{Im}(k_2)\leq\operatorname{Im}(k_3)\leq\operatorname{Im}(k_4)$. In our case, the "absolute spectrum" is the set of λ such that $\operatorname{Im}(k_2)=\operatorname{Im}(k_3)$, and $\lambda_{\max}(V)$ is the λ in the absolute spectrum with maximum real part. "Branch points" are the six values of λ such that $k_i=k_i+1$, and they are used as starting points for numerical continuation to obtain the full "generalised absolute spectrum" [22]. For $\lambda_{\max}(V)$ however, one need only consider branch points in the absolute spectrum ($k_2=k_3$)—it can be assumed that the λ in the absolute spectrum with maximum real part coincides with a branch point, vastly reducing the computation. One simply obtains all branch points (solutions of $\mathcal{D}(\lambda,k;V)=\mathcal{D}_k(\lambda,k;V)=0$) along with corresponding k_i; retaining those λ with $\max\operatorname{Re}(\lambda)$ for which $k_2=k_3$. It has been proved that the most unstable point in the absolute spectrum is a branch point in the case of the λ-ω equations [23], however, we are not aware of a proof for the CGLE case, and indeed numerical evidence [22] suggests this is not true for all parameters. Moreover, these cases would not be relevant in this paper since they correspond to "remnant instabilities" which are not significant when studying bands of PTWs [24].

3. Implications for the predator–prey model

We performed numerical simulations for various β in order to vary $\mathcal{W}$ and confirm its linear relationship with the observed band width which we show in Fig. 2(a). This allows one to calculate $\log(\mathcal{F})$ which we do using a simple linear regression; this only needs applying once and indeed one can reuse our calculated value when changing parameters in (1)—in this paper we obtain $\log(\mathcal{F})=29.77$. We tested our predictions of $\mathcal{W}$ by solving (1) using a semi-implicit finite difference scheme and computing the band width by viewing the solution as $r=\sqrt{\operatorname{Re}(W)^2+\operatorname{Im}(W)^2}$; we defined the band by the condition $|\partial r/\partial x|<1\times10^{-3}$. We estimated the derivative numerically after applying a Savitzky–Golay smoothing algorithm over a moving window of 9 grid points. The band width obtained by using this threshold is slightly smaller than that observed by visual inspection, and is simply due to the threshold one chooses, which affects the calculated end points of the band of PTWs. This has implications for the best-fit line shown in Fig. 2(a) in which we observe a non-zero intercept in the regression line. This can be attributed to the excluded regions on either side of our numerically calculated band width.

We apply our results to the following specific functional forms

$$f(p,h)=cp\left(1-\frac{p}{h}\right), \qquad g(p,h)=h(1-h)-\frac{aph}{b+h}, \tag{5}$$

which makes (1) the Leslie–May model [25,26]. The methodology described in this paper is however applicable to any model of the form (1) that undergoes a standard supercritical Hopf bifurcation as a parameter is varied. Since the parameter δ is our primary focus we refer the reader to, for example, [27, Chapter 3.4] for a full description of the non-dimensional parameters: $a>0$, $b>0$, $c>0$. Taking (5) in (1) yields the prey-only steady state $(p,h)=(0,1)$, and two coexistence steady states given by

$$p_\pm=\frac{1}{2}\left(1-a-b\pm\sqrt{((1-a-b)^2+4b)}\right), \qquad h_\pm=p_\pm. \tag{6}$$

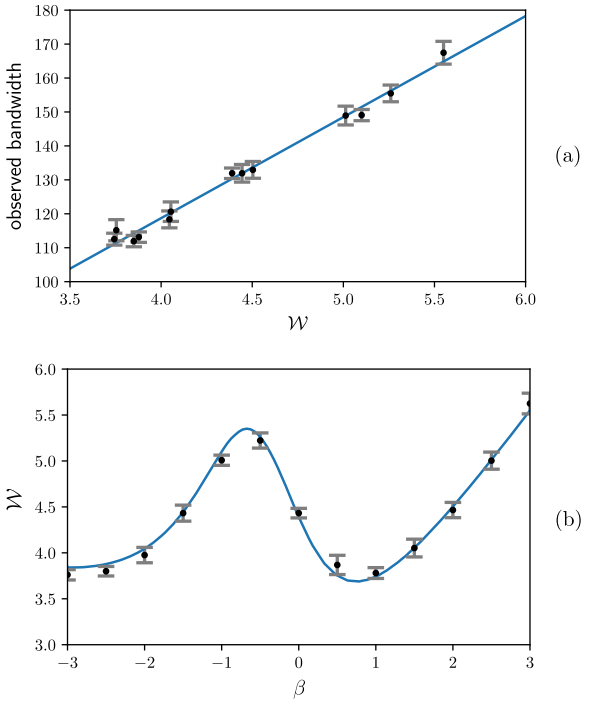

Fig. 2. Comparison of the band width coefficient $\mathcal{W}$ with numerical simulation of (2), with $\alpha = 3$. The points and error bars are the mean and standard deviation of a sample of 500 numerically computed band width estimations at distinct time points spaced 0.2 time units apart. In (a) we plot $\mathcal{W}$ against the numerically computed band width and perform a simple linear regression. The line of best fit has slope $\log \mathcal{F} = 29.77$, intercept -0.36, and has a correlation coefficient of 0.9946. In (b) the same data points are rescaled using the linear regression constants and the line is the predicted band width coefficient calculated numerically using the method described in the main text.

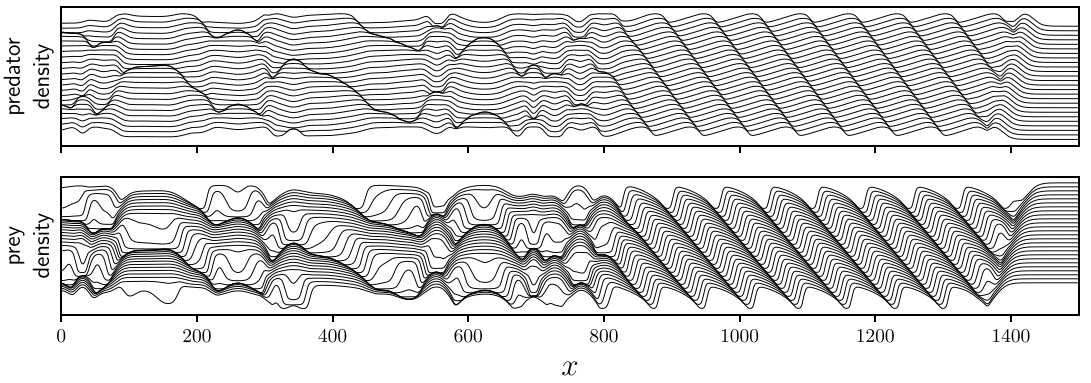

Fig. 3. Convectively unstable periodic travelling waves generated by an invasion in a cyclic predator–prey interaction. The solution is plotted at equally spaced time intervals in the range $3099.5 \leq t \leq 3200$, with successive plots layered above and behind one another. This visualisation reveals an invasion front moving towards the right boundary, behind which a band of PTWs moves towards the left, eventually destabilising as a result of a convective instability. Eq. (1) with (5) was solved using a semi-implicit finite difference scheme with a grid spacing of 0.2 and a time step of 0.005, on a domain with zero flux boundary conditions at both ends. Parameters are $\delta = 0.8$, $a = 0.77$, $b = 0.08$, $c = 0.0517$. Note that the band of PTWs in this figure is still growing and has not yet reached its fixed band width.

An invasion of predators into the unstable steady state is shown in Fig. 3; similarly to the CGLE one observes a band of PTWs behind an invasion front, and spatio-temporal irregularity thereafter.

The first step in determining the band width of PTWs in a predator–prey model is to calculate α and β in terms of the model parameters. In this paper we are concerned with the effect that predator and prey dispersal rates have on the band width via the parameter δ. For models of the form (1) α is always

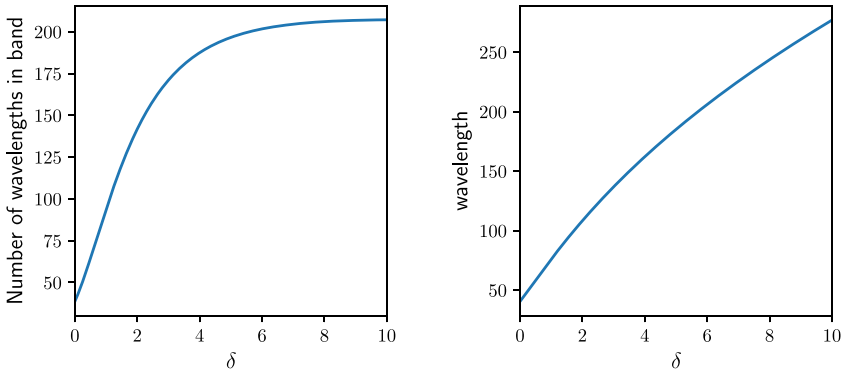

Fig. 4. Our predicted band width as a function of the ratio of prey and predator dispersal rates δ. In (a) we plot the number of wavelengths observed in the PTW band, and in (b) we plot the wavelength of the PTWs in the band. Parameters in the original model are $a = 0.72$, $b = 0.06$ and we set $c = c_{\text{crit}} - 0.05$.

independent of δ. We take c to be a control parameter: by fixing $a = 0.72$, $b = 0.06$ we obtain the Hopf bifurcation point $c = c_{\text{crit}} \approx 0.158$ which gives the normal form coefficient $\alpha = 1.441$. By fixing these parameters β is now solely determined by δ. We show how δ affects band width by plotting the number of wavelengths observed in the band in Fig. 4(a), along with the associated wavelength in Fig. 4(b); this is given by $2\pi/(1 - A^2)$ subject to normal form rescalings. Note that $\delta < 1$ corresponds to a system in which predators disperse at a higher rate than their prey, and vice-versa for $\delta > 1$. We find that a higher predator dispersal rate shortens the band width by reducing both the wavelength of PTWs and the number of oscillations observed in the band. One therefore concludes that an increased predator dispersal rate has a destabilising effect on the regular oscillations behind an invasion front. In contrast an increased prey dispersal rate increases the band width observed. For larger δ one obtains an absolutely stable solution where irregular behaviour is not observed, whereas for smaller δ one obtains an absolutely unstable solution where no PTWs are observed (not shown in Fig. 4). Therefore our results are in accordance with what one would expect from absolute stability theory—PTWs that are close to being absolutely stable will have a longer band width, whereas PTWs close to being absolutely unstable will have a shorter band width.

4. Discussion

We considered the PTWs generated by an invasion in a cyclic predator–prey system. For certain parameter values, the PTWs are convectively unstable, which means a fixed width band of PTWs is observed before irregular oscillations. We combine theory developed in [15,17] with a recent equation for the amplitude of PTWs [18] to determine how predator and prey dispersal affects the band width of PTWs. By applying the methodology to the Leslie–May model, we find a monotonically increasing relationship between the ratio of prey to predator dispersal rates and the band width—see Fig. 4. A large predator (or small prey) dispersal rate will therefore have a destabilising effect on spatio-temporal oscillations and a shorter band width will be observed. Similarly a large prey (or small predator) dispersal rate will lead to a larger band width. We emphasise that the approximation described in this paper requires proximity to a standard supercritical Hopf bifurcation point, and therefore is only valid for small amplitude PTWs.

Though we have drawn conclusions based on the Leslie–May model, Fig. 2(b) suggests that a monotonic relationship between the dispersal rate and band width may not always be the case. A different model and parameters will generate different normal form coefficients, and consequently there may be instances, for example, where an increase/decrease in band width will be observed regardless of the direction in which δ varies. One may also note that for our chosen model we obtain very long band widths—much longer

than any realistic habitat for all δ considered. This suggests that for practical purposes one need only consider two cases, namely where the PTWs are absolutely stable (uninterrupted PTWs) or absolutely unstable (spatio-temporal irregularity observed immediately behind invasion). Of course, consideration of a different model may reveal shorter band widths that have more significance, however, previous work [15] that applies the methodology described in this paper to the Rosenzweig–MacArthur model with equal dispersal coefficients [28] reaches a similar conclusion.

References

[1] J.J. Hellmann, J.E. Byers, B.G. Bierwagen, J.S. Dukes, Five potential consequences of climate change for invasive species, Conserv. Biol. 22 (3) (2008) 534–543.
[2] T.S. Doherty, A.S. Glen, D.G. Nimmo, E.G. Ritchie, C.R. Dickman, Invasive predators and global biodiversity loss, Proc. Natl. Acad. Sci. USA 113 (40) (2016) 11261–11265.
[3] J.A. Sherratt, M.J. Smith, Periodic travelling waves in cyclic populations: field studies and reaction–diffusion models, J. R. Soc. Interface 5 (22) (2008) 483–505.
[4] S.M. Merchant, W. Nagata, Wave train selection behind invasion fronts in reaction-diffusion predator-prey models, Physica D 239 (2010) 1670–1680.
[5] S.M. Merchant, W. Nagata, Instabilities and spatiotemporal patterns behind predator invasions with nonlocal prey competition, Theor. Popul. Biol. 80 (4) (2011) 289–297.
[6] S. Petrovskii, M. Vinogradov, A.Y. Morozov, Spatial-temporal dynamics of a localized populational "burst" in a distributed prey-predator system, Okeanologiya 38 (6) (1998) 881–890.
[7] F. Davidson, Chaotic wakes and other wave-induced behavior in a system of reaction–diffusion equations, Int. J. Bifurcation Chaos 8 (06) (1998) 1303–1313.
[8] S.V. Petrovskii, H. Malchow, Critical phenomena in plankton communities: KISS model revisited, Nonlinear Anal. RWA 1 (1) (2000) 37–51.
[9] S.V. Petrovskii, H. Malchow, Wave of chaos: new mechanism of pattern formation in spatio-temporal population dynamics, Theor. Popul. Biol. 59 (2) (2001) 157–174.
[10] M.R. Garvie, Finite-difference schemes for reaction–diffusion equations modeling predator–prey interactions in MATLAB, Bull. math. biol. 69 (3) (2007) 931–956.
[11] M.R. Garvie, J. Burkardt, J. Morgan, Simple finite element methods for approximating predator–prey dynamics in two dimensions using matlab, Bull. Math. Biol. 77 (3) (2015) 548–578.
[12] M. Banerjee, S. Petrovskii, Self-organised spatial patterns and chaos in a ratio-dependent predator–prey system, Theor. Ecol. 4 (1) (2011) 37–53.
[13] J.A. Sherratt, Periodic travelling waves in cyclic predator prey systems, Ecol. Lett. 4 (2001) 30–37.
[14] N. Kopell, L.N. Howard, Plane wave solutions to reaction-diffusion equations, Stud. Appl. Math. 52 (1973) 291–328.
[15] J.A. Sherratt, M.J. Smith, J.D.M. Rademacher, Locating the transition from periodic oscillations to spatiotemporal chaos in the wake of invasion, Proc. Natl. Acad. Sci. USA 106 (2009) 10890–10895.
[16] J.A. Sherratt, On the evolution of periodic plane waves in reaction-diffusion equations of λ-ω type, SIAM J. Appl. Math. 54 (1994) 1374–1385.
[17] M.J. Smith, J.A. Sherratt, Propagating fronts in the complex Ginzburg-Landau equation generate fixed-width bands of plane waves, Phys. Rev. E 80 (4) (2009) 046209.
[18] J.J.R. Bennett, J.A. Sherratt, Periodic traveling waves generated by invasion in cyclic predator–prey systems: The effect of unequal dispersal, SIAM J. Appl. Math. 77 (6) (2017) 2136–2155.
[19] W. van Saarloos, Front propagation into unstable states, Phys. Rep. 386 (2003) 29–222.
[20] A.S. Dagbovie, J.A. Sherratt, Absolute stability and dynamical stabilisation in predator-prey systems, J. Math. Biol. 68 (6) (2014) 1403–1421.
[21] J.A. Sherratt, A.S. Dagbovie, F.M. Hilker, A mathematical biologist's guide to absolute and convective instability, Bull. Math. Biol. 76 (1) (2014) 1–26.
[22] J. Rademacher, B. Sandstede, A. Scheel, Computing absolute and essential spectra using continuation, Physica D 229 (2007) 166–183.
[23] M.J. Smith, J.D. Rademacher, J.A. Sherratt, Absolute stability of wavetrains can explain spatiotemporal dynamics in reaction-diffusion systems of lambda-omega type, SIAM J. Appl. Dyn. Syst. 8 (3) (2009) 1136–1159.
[24] B. Sandstede, A. Scheel, Absolute and convective instabilities of waves on unbounded and large bounded domains, Physica D 145 (2000) 233–277.
[25] P.H. Leslie, Some further notes on the use of matrices in population dynamics, Biometrika 35 (1948) 213–245.
[26] R. May, Stability and Complexity in Model Ecosystems, Princeton University Press, 1974.
[27] J.D. Murray, Mathematical Biology I : An Introduction, Springer, 2002.
[28] M.L. Rosenzweig, R.H. MacArthur, Graphical representation and stability conditions of predator-prey interactions, Am. Nat. 97 (895) (1963) 209–223.